Synthesis and Properties of a Visible-to-Near-IR-Fluorescing 2,5-Diarylidene Cyclopentanone Charge-Transfer Dye

A MAJOR QUALIFYING PROJECT

Submitted to the Faculty of the

WORCESTER POLYTECHNIC INSTITUTE

in partial fulfillment of the requirements for the

Degree of Bachelor of Science

By

_____

Zhen Chen

Date: May 3, 2010

_____

Dr. Robert E. Connors, Advisor

Abstract

A conjugated dye, (*2E,5E*)-2-[(4-cyanophenyl)methylene]-5-[(*E*)-3-[4-(dimethylamino)phenyl]-2-propen-1-ylidene]-cyclopentanone, was synthesized. Absorption and fluorescence emission were measured in various solvents; enlarged Stokes shifts in increasingly polar solvents were observed. This, along with TD-DFT calculations, proved the charge-transfer nature of the S_1 state. Solvent effect on the dye's fluorescence quantum yield and lifetime was measured; the largest values of both were observed in chloroform. Trends were explained by rate constants of fluorescence and non-radiative decay, structure of electronic states, and transitions among them. Finally, the two-photon absorption cross-section of the molecule was calculated. The large value suggested its potential use as a two-photon dye.

Acknowledgements

I would like to thank Professor Robert E. Connors for the use of his laboratory and for his help and guidance throughout the project, and graduate student Chris Zoto for helpful discussions and detailed instructions on laboratory operations.

Contents

List of Figures

List of Tables

Introduction

Organic compounds containing chains of conjugated unsaturated bonds have excited electronic states that are relatively low in energy. As a result, they are often dyes that absorb and emit photons within or near the visible range. Chemists describe those processes by Jabłoński diagrams such as Figure 1, where commonly encountered transitions between the energy states of a molecule are illustrated.

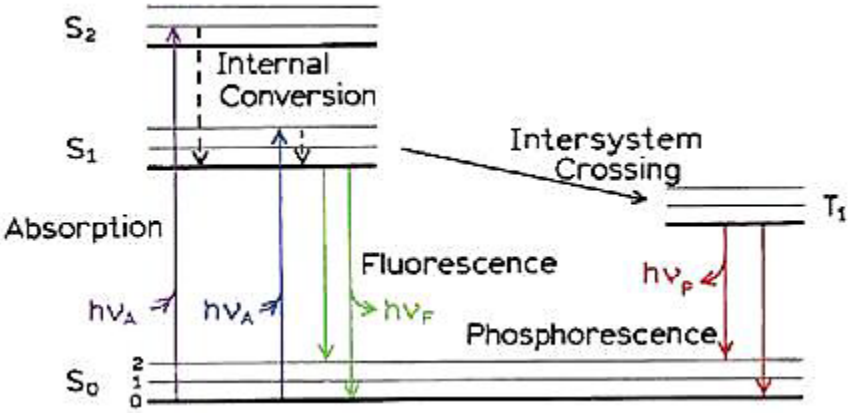

Figure 1. Jabłoński diagram of commonly encountered transitions between energy states of a molecule.[i]

Starting from the singlet ground state, a molecule may absorb a photon and be promoted into an excited singlet state. If it is promoted into a high excited state, it undergoes rapid non-photon-emitting (so-called "non-radiative") internal conversion and reaches the lowest excited state. There are a few possibilities at this point. The molecule may emit a photon and go back to the ground state, which is known as fluorescence. It may go through a further internal conversion and return to the ground state non-radiatively. Or it may go through an intersystem crossing (a non-radiative process) and reach an excited triplet state, where it can then either emit a photon (known as phosphorescence) or lose its remaining energy non-radiatively.

[i] Image source: Joseph R. Lakowicz, Principles of Fluorescence Spectroscopy, 3rd ed. (New York: Springer, 2006), 5.

The percentage of absorbed photons that ultimately lead to fluorescence is called the fluorescence quantum yield. When fluorescence is monitored over time (usually on the scale of nanoseconds), an exponential decay is often observed. The time constant is called the fluorescence lifetime. Quantum yield and lifetime are the principal photophysical properties of a fluorescent molecule in a certain environment. Phosphorescence of organic molecules is rarely observed in solutions at room temperature. Information about the non-radiative processes is difficult to obtain experimentally, but can be inferred from the above two fluorescence parameters.[1]

Our research group has developed many dye molecules whose structures contain a carbonyl group connecting two conjugated chains.[2,3] Recently Zoto and Connors reported the properties of a "push-pull" dye, one that has an electron-donating substituent on one end and an electron-withdrawing substituent on the other.[3] Interest in such molecules arises from their electronic structure. In the case of the molecule in Ref. 3, the highest occupied molecular orbital (HOMO) has high electron density closer to the electron-donating end, while the lowest unoccupied molecular orbital (LUMO) has high electron density at the electron-withdrawing end. Therefore, promotion of a HOMO electron into the LUMO dramatically changes the charge distribution throughout the molecule, producing an internal-charge-transfer (ICT) state. Dyes with this feature have been used to design materials with high second-harmonic generation (SHG) or two-photon absorption (TPA) intensities.[4]

In addition, the spectroscopic and photophysical behavior of these molecules changes drastically with solvent polarity. The general mechanism of solvent effect is shown in Figure 2. At its lowest excited electronic state, a dye molecule has a relatively long lifetime (on the order of 10^{-9} s). This is enough time for solvent molecules surrounding it to reorient their dipoles and relax, which lowers the energy of the system before fluorescence takes place. Two implications of this phenomenon can be experimentally observed. First, the photon emitted by fluorescence would be lower in energy ("red-shifted"). Increased

polarity of either the solvent or the dye magnifies this effect, so a molecule that exhibits large dipole moments in its lowest excited state, such as "push-pull" molecules, will fluoresce at much red-shifted wavelengths in polar solvents than in nonpolar solvents (a phenomenon known as "solvatochromism"). This implies possible application of these dyes as polarity probes or ion sensors. Secondly, solvent-induced change in energy levels (including ground state, excited singlet states, and excited triplet states) alter the energy gaps, and sometimes even the order, among those levels. This affects kinetic parameters of photophysical processes.[1] [ii]

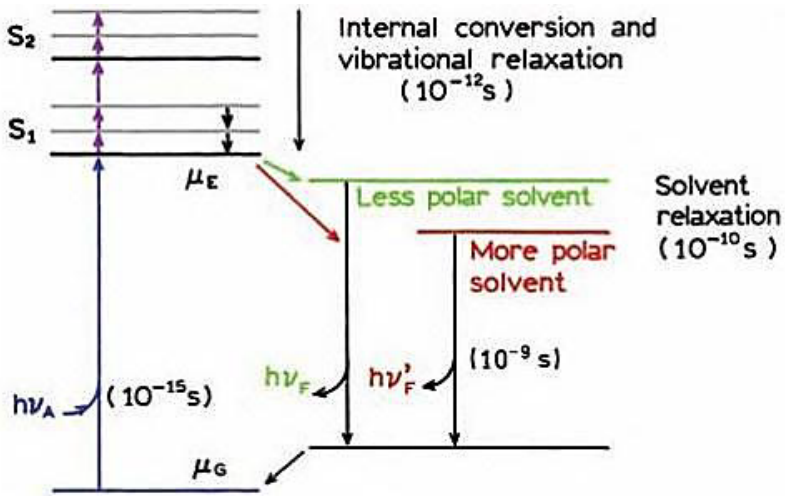

Figure 2. Jabłoński diagram illustrating the mechanism of solvent effect on spectroscopic and photophysical behavior of dye molecules.[iii]

This project focused on synthesizing and characterizing a molecule that is longer than the published dye by one conjugated double bond unit (Figure 3). The effect of conjugation chain length on a dye's spectroscopic properties can be qualitatively determined by a "particle-in-a-box" model. In this model, a loosely-bound electron in a conjugated system is approximated as a free particle in a one-dimensional potential energy well with infinitely high walls. It can be shown in quantum mechanics that

[ii] This simple treatment is usually valid when the first excited state in question is a π,π* state, which is often true for charge-transfer molecules. The conclusions may not hold, however, for dyes of other electronic configurations.
[iii] Image source: Joseph R. Lakowicz, *Principles of Fluorescence Spectroscopy*, 3rd ed. (New York: Springer, 2006), 206.

the particle can only have discrete energy levels. Furthermore, the energy difference between the ground state and the first excited state is inversely proportional to the square of the width of the well. So a wider well, or analogously a longer chain, results in a lower-lying excited state. Therefore, it can be expected that the dye reported in this project absorbs and emits at lower wavenumbers, or longer wavelengths, than the previously published one.

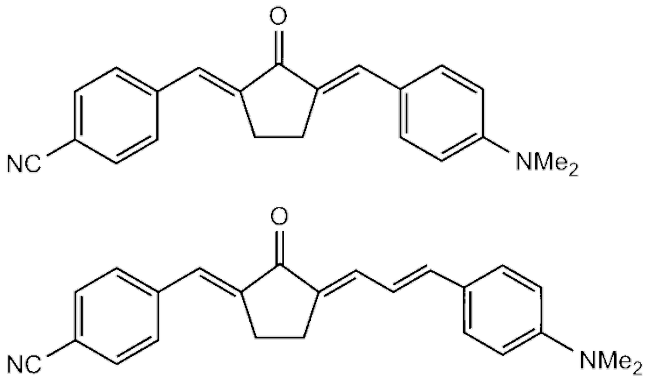

1

Figure 3. (Top) The push-pull dye studied in Ref. 3. (Bottom) The analogous dye **1** studied in this project.

The possibility of applying compound **1** as a two-photon dye was briefly explored in this project by computational methods. Two-photon absorption is excitation of a molecule by absorption of two photons in one process. It offers higher resolution or accuracy than one-photon absorption for many optical applications, such as three-dimensional microfabrication, optical data storage, optical limiters, photodynamic therapy, and fluorescence microscopy. Design of efficient two-photon dyes is therefore highly desirable.[5]

Methods

General

UV-visible spectra were obtained on a PerkinElmer Lambda 35 UV/VIS spectrometer with 2 nm band-passes. Fluorescence emission spectra were obtained on a PerkinElmer LS 50B luminescence spectrophotometer equipped with a R928 phototube detector. Fluorescence lifetime was measured on a Photon Technology International TM-3A/2005 system. For all absorption and fluorescence measurements, solvents were spectrophotometric grade or HPLC grade except for the following: cyclopentanone, dichloromethane, ethyl acetate, ethanol, *n*-butanol, and 1,2-dichlorobenzene. All cuvettes have a path length of 1 cm. NMR spectra were obtained on a Bruker AVANCE 400MHz spectrometer. Theoretical calculations were performed using Gaussian 09[6], except for two-photon absorption calculations, which were performed with Dalton 2.0.[7]

Synthesis of (*E*)-2-(*p*-cyanobenzylidene)cyclopentanone 1dbcn

Approach 1[8]

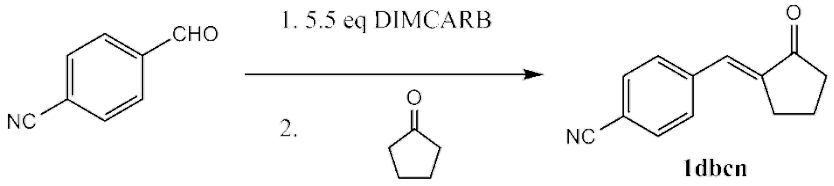

1dbcn

In 15 ml chloroform was dissolved 1.312 g (10 mmol) *p*-cyanobenzaldehyde. Dimethylammonium *N,N*-dimethylcarbamate ("DIMCARB"; 7.2 ml, 55 mmol) was added dropwise with constant stirring. Gas was evolved. Cyclopentanone (0.885 ml, 10 mmol) was added in one portion. The solution was stirred at room temperature until no trace of the benzaldehyde was observed on TLC. The

mixture was concentrated under reduced pressure to become a sticky brown fluid, which was taken up in 20 ml 0.5 M sulfuric acid. The mixture was extracted by 3×20 ml dichloromethane, and the organic portion was dried overnight. The product was then isolated by column chromatography (gradient hexane/ethyl acetate). The reaction was repeated with dichloromethane as the solvent, or with four days of stirring. Traces of the material that had the same signals as described in the literature were seen in the NMR, but yield was low.

Approach 2[9]

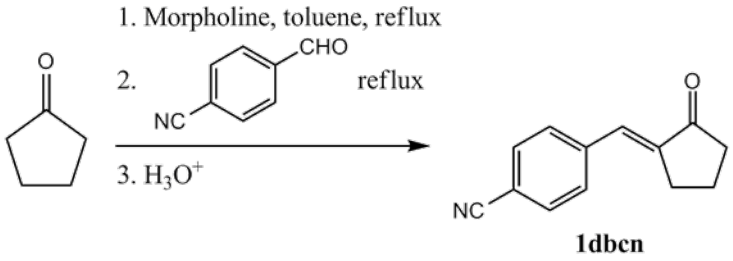

1dbcn

Morpholine (0.97 ml, 0.01 mol) was dissolved in toluene (10 ml). Cyclopentanone (0.885 ml, 0.01 mol) was added with stirring, and the mixture was refluxed for 15 minutes. After cooling, *p*-cyanobenzaldehyde (1.310 g, 0.01 mol) was added with stirring, and the mixture was refluxed for 2 hours. After cooling, a 1:1 mixture of water and concentrated HCl (5 ml) was added. The mixture was stirred for an hour, and then repeatedly washed with 10% aqueous $NaHCO_3$ until no gas evolved. The organic layer was concentrated unter reduced pressure to give a deep-brown solid. The reaction was repeated, but with 3 hours of reflux both before and after the addition of p-cyanobenzaldehyde. The two portions combined were purified by column chromatography (gradient hexane/ethyl acetate), where 1.5 g (38%) of the product was collected in acceptable purity as judged by NMR. Some of the material was recrystallized from CH_2Cl_2/hexanes to give a lightly yellow crystal. mp. 113-114 °C (lit.[9] 112-113) ^{1}H-NMR ($CDCl_3$): 2.01 (qn, J 7.6), 2.38 (t, J 7.6, 2H), 2.92 (td, J 7.2, 2H), 7.28 (t, J 2.8, 1H), 7.54 (d, J 8.3, 2H), 7.65 (d, J 8.4, 2H).

Synthesis of (*2E,5E*)-2-[(4-cyanophenyl)methylene]-5-[(*E*)-3-[4-(dimethylamino)phenyl]-2-propen-1-ylidene]-cyclopentanone 1[3]

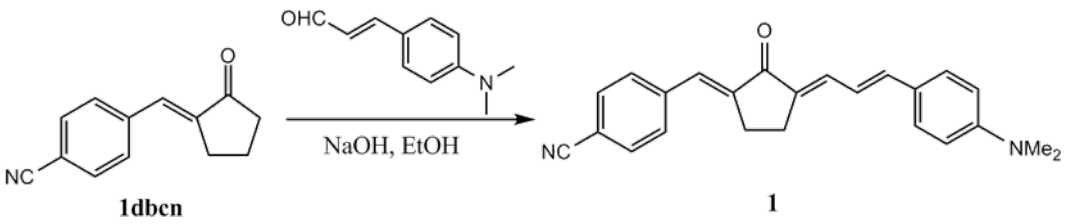

1dbcn **1**

4-(Dimethylamino)cinnamaldehyde (0.350 g, 0.002 mol) was dissolved in a minimum amount of ethanol (100 ml). An aqueous solution of NaOH (2.5% w/v, 1ml) was added, and the solution was stirred in ice bath. With constant stirring, a solution of **1dbcn** (0.395 g, 0.002 mol) in a minimum amount of ethanol (25 ml) was added dropwise. When the addition was complete, the mixture was immediately filtered to give 80 mg of a deep purple solid (compound **1**). The filtrate was stored in a freezer overnight and was filtered while cold, where 150 mg of the same solid was collected. Water was added to the filtrate, and a further 50 mg of the same solid was collected by filtration. Total crude yield was 39%. The solids were recrystallized from CH_2Cl_2/hexanes to give deep purple small flaky crystals. Thermal behavior: decomposed 230-250 °C before melting. ^{1}H-NMR ($CDCl_3$): 2.96 (sharp s superimposed on wide m, 10H), 6.60 (d, J 8.8, 2H), 6.70 (dd, J 12, 1H), 6.92 (d, J 15, 1H), 7.33 (m, J 12, 4H), 7.60 (q, J 22, 4H).

Acquiring and correcting fluorescence emission spectra[1]

Fluorescence emission spectra were acquired with excitation wavelength set at 470 nm, except for the spectrum of **1** in *n*-hexane, for which the excitation wavelength was 430 nm. Before correction, all spectra were converted to the wavenumber scale, and signals corresponding to scattered excitation light were removed. The spectra were corrected for the different instrument response at different

wavelengths in the following way: Published standard solutions, namely (a) a 10^{-4} M solution of *N,N*-dimethylamino-*m*-nitrobenzene in 30% benzene/70% *n*-hexane and (b) a dilute solution of 4-dimethylamino-4'-nitrostilbene in *o*-dichlorobenzene, were prepared, and their fluorescence emission spectra were taken on the specific instrument used in this project. The obtained spectra were converted to the wavenumber scale, compared to published corrected spectra, and correction factors were obtained for the range of interest.

Extrapolation of fluorescence emission spectra

Corrected fluorescence emission spectra of compound **1** in the following solvents were extrapolated into regions that are smaller in wavenumber than the detection limit of the instrumentation: acetone, tetrahydrofuran, acetonitrile, pyridine, and cyclopentanone. For each of those, correction was achieved by shifting the spectrum of **1** in benzene and adjusting the intensity at every wavenumber by a constant factor, such that the peaks of the two spectra coincided.

Fluorescence quantum yield[10]

Fluorescence quantum yield was measured using a comparative method against the fluorescein standard. Fluorescein was dissolved in 0.1 N NaOH and diluted such that its absorbance was approximately 0.5 at 470 nm. The absorbance was recorded. The solution was then accurately diluted tenfold. A fluorescence emission spectrum was taken, converted to the wavenumber scale, corrected, and integrated. The series of operations was repeated for compound **1** dissolved in the solvent of interest. The fluorescence quantum yield of **1** in that solvent was calculated according to

$$\Phi_f = \Phi_{f,std} \cdot \frac{A_{std}}{A} \cdot \frac{n^2}{n_{std}^2} \cdot \frac{D}{D_{std}}$$

where Φ_f is fluorescence quantum yield ($\Phi_{f,std}$ = 0.95[1]), A is the absorbance at the excitation wavelength, n is the refractive index of the solvent, and D is the area under the corrected, extrapolated emission spectra.

Fluorescence lifetime

Samples for fluorescence lifetime were prepared by dissolving compound **1** in the solvent of interest to absorbance < 0.05 and degassing with nitrogen gas. The measured decay curve was analyzed against an instrument response function (IRF) obtained from LUDOX (colloidal silica suspension in water) assuming a single exponential decay.

Theoretical calculations

The geometry was optimized in gas phase using Density Functional Theory (DFT) at the B3LYP/6-311+G(d) level of theory. All subsequent calculations used this structure. Molecular orbitals and electronic states in gas-phase, chloroform, and carbon tetrachloride, as well as the room-temperature UV-visible spectrum in chloroform, were calculated with time-dependent DFT (TD-DFT) at the B3LYP/6-311+G(d,p) level of theory. Two-photon absorption cross-section was calculated only in gas phase at the B3LYP/cc-pVDZ level of theory, following a procedure available in the literature.[4]

Results and Discussion

Structural and spectroscopic properties

The structure of compound **1**, determined by computation in gas phase, was found to be nearly planar, with some twisting at the central cyclopentanone ring (Figure 4). The dihedral angle between the two aromatic rings is 18 degrees. The ground state dipole moment is 12.5 D. The Onsager cavity radius, an indication of the volume occupied the molecule in a dielectric medium (such as solution phase), is 5.83 Å.

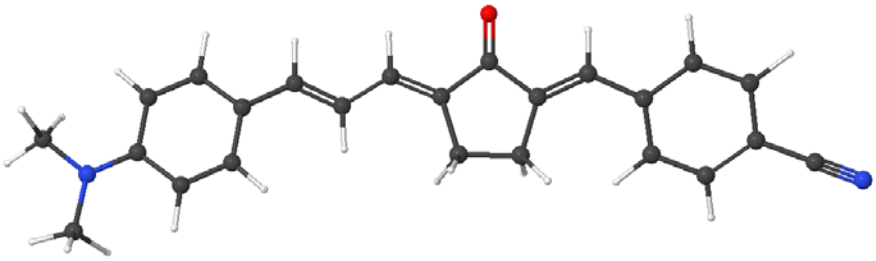

Figure 4. Structure of compound **1** from gas-phase theoretical calculations.

Based on the structure, molecular orbitals were calculated in gas phase, and the orbitals relevant to electronic transitions are shown in Figure 5. It can be seen that the HOMO has large electron density near the dimethylamino end (i.e. the electron-donating end), while electron density of the LUMO is located closer to the cyano end and the central carbonyl oxygen (i.e. the electron-withdrawing parts). LUMO+1 has its electron density further to the cyano end. HOMO-1 is a more localized π orbital, while HOMO-2 and HOMO-3 are non-bonding orbitals.

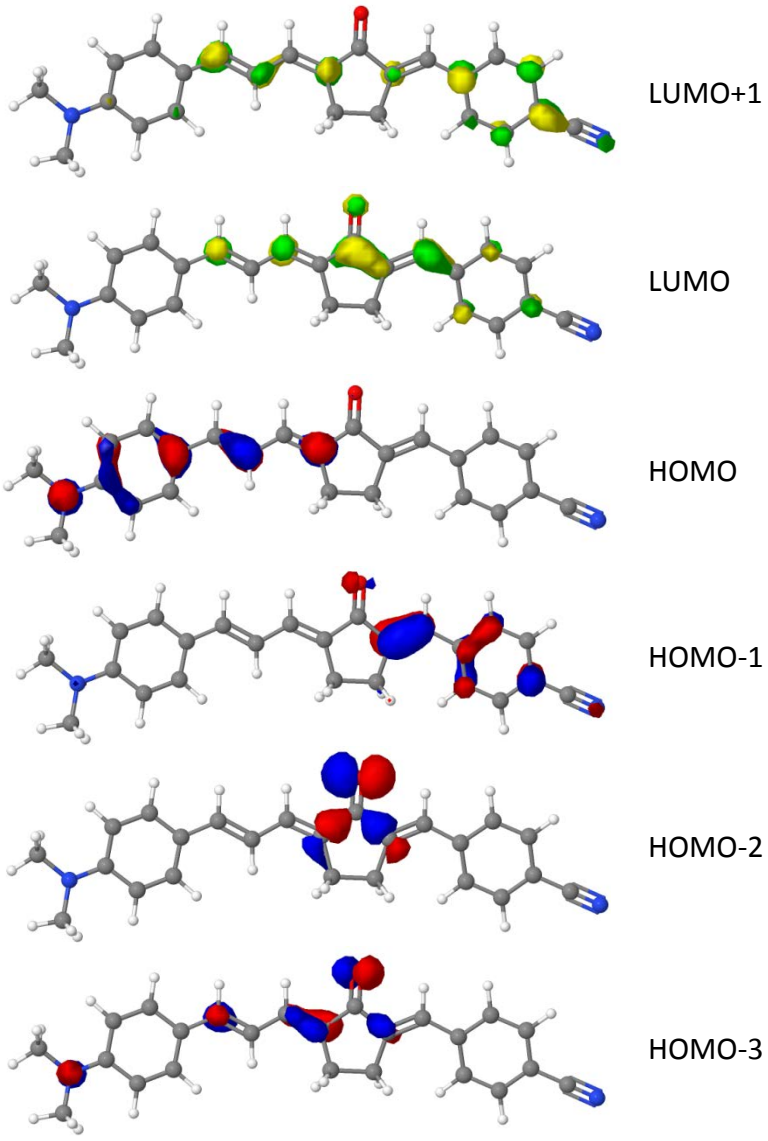

Figure 5. Molecular orbitals of compound **1**, calculated in gas-phase using TD-DFT. Red and blue lobes represent occupied orbitals. Green and yellow lobes represent unoccupied orbitals.

Electronic excitations were then calculated using chloroform as the implicit solvent. Results indicate that the lowest excitation, predicted to occur at 562 nm, is a strong π,π* transition from S_0 to S_1, where one electron was promoted from the HOMO to the LUMO. As discussed above, the two orbitals are different in the location of electron density, and therefore this promotion results in an internal charge transfer (ICT) state. The next excitation, S_0 to S_2 at 417 nm, is a forbidden n, π* excitation

arising from HOMO-3 -> LUMO and HOMO-2 -> LUMO. The third excitation, S_0 to S_3 at 390 nm, is a mixture of the charge-transfer HOMO -> LUMO+1 and the localized excitation HOMO-1 -> LUMO. The overall nature of the transition is π,π*. It is weaker than the first excitation.

The UV-visible spectrum of compound **1** in chloroform was obtained, and a qualitative agreement with the excitation calculations can be observed in Figure 6. Specifically, the band that peaks at 498 nm corresponds to the S_0 -> S_1 transition, whereas the band that peaks at 339 nm corresponds to the S_0 -> S_3 transition. The forbidden S_0 -> S_2 transition was not observed. The relative intensities of the peaks were also the same as predicted.

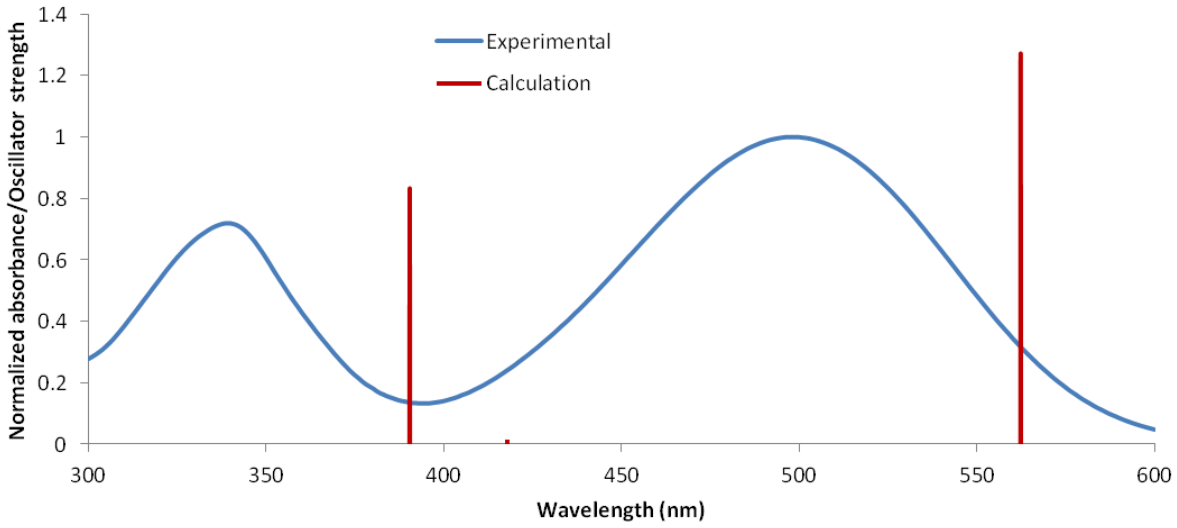

Figure 6. (Blue) UV-visible spectrum of compound **1** in chloroform. (Red) Electronic excitations calculated with chloroform as the implicit solvent using TD-DFT. A qualitative agreement can be seen.

The UV-visible spectra of **1** in various other solvents were also obtained. Absorption maxima are listed in Table 1; selected spectra are given in Figure 7. As solvent polarity increases, the absorption maximum generally red-shifts from 474 nm to 500 nm, but the trend is not monotonous. The absorption band in alcohols is much broader than that in all other solvents. The absorption band corresponding to

the S_0 to S_3 transition, if not obscured by the solvent's own absorption, appears between 330 nm and 350 nm.

Table 1. Spectroscopic properties of compound **1** in various solvents. Solvent polarity [$E_T(30)$ and Δf] is also listed.

Solvent	$\lambda_{max,abs}$ (nm)	$\tilde{\nu}_{max,abs}$ (cm^{-1})[a]	$\tilde{\nu}_{max,f}$ (cm^{-1})[b]	Stokes shift (cm^{-1})	$E_T(30)$	Δf
Carbon tetrachloride	477	20964	16800	4164	32.4	0.0119
Carbon disulfide	497	20121	16050	4071	32.8	-0.0007
Toluene	481	20790	15900	4890	33.9	0.0131
Benzene	485	20619	15850	4769	34.3	0.0031
Tetrahydrofuran	478	20921	14600	6321	37.4	0.2104
o-Dichlorobenzene	498	20080	14700	5380	38.0	0.1867
Ethyl acetate	474	21097	14450	6647	38.1	0.1996
n-Butyl acetate	474	21097	15050	6047	38.5	0.1709
Chloroform	497	20121	14950	5171	39.1	0.1491
Cyclopentanone	486	20576	13350	7226	39.4	0.2391
Pyridine	496	20161	13300	6861	40.5	0.2124
Dichloromethane	492	20325	14250	6075	40.7	0.2171
Acetone	478	20921	13200	7721	42.2	0.2843
Dimethylformamide	489	20450	12850	7600	43.2	0.2752
Dimethyl sulfoxide	500	20000	12650	7350	45.1	0.2637
Acetonitrile	480	20833	12900	7933	45.6	0.3054
Isopropanol	500	20000	13500	6500	48.4	0.2769
n-Butanol	504	19841	13650	6191	50.2	0.2642
n-Propanol	502	19920	13550	6370	50.7	0.2746
Ethanol	500	20000	13300	6700	51.9	0.2887
Methanol	499	20040	13050	6990	55.4	0.3093

[a] Converted directly from $\lambda_{max,abs}$.

[b] Obtained from corrected spectra.

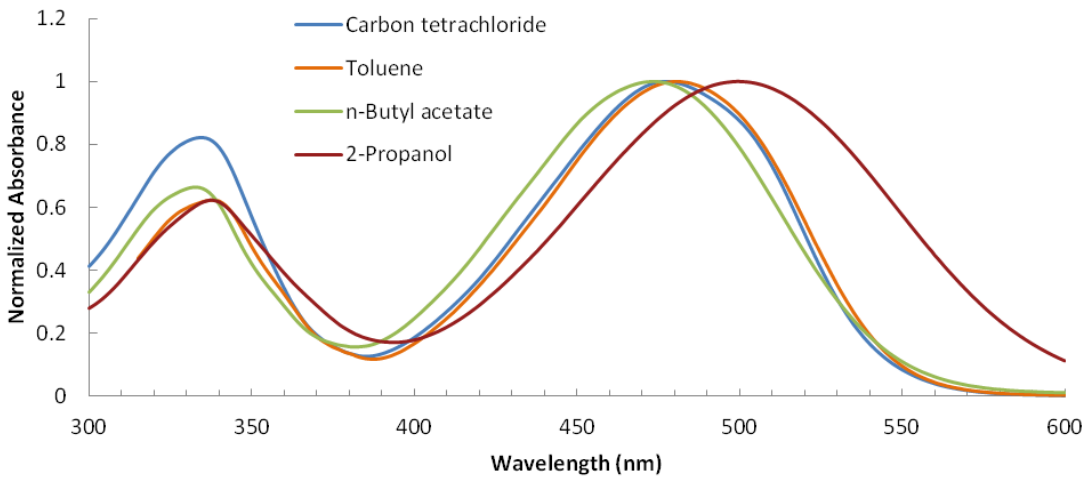

Figure 7. UV-visible spectra of compound **1** in various solvents.

Fluorescence emission spectra of compound **1** in various solvents exhibit some interesting variations (Figure 8). In *n*-hexane, two distinct peaks appear at 19750 cm^{-1} and 18250 cm^{-1}. The peaks can be associated with transitions from the lowest vibrational state within the S_1 state to two different vibrational states within the S_0 state. In CCl_4 and CS_2, the peaks broaden, and the lower-intensity peak only appears on the shoulder of the higher-intensity one. As solvent polarity further increases, the spectra all contain only one broad band. The polarity-dependent red-shift in emission maxima ("solvatochromism") is much more pronounced than that in absorption maxima. For a few polar aprotic solvents – acetone, tetrahydrofuran, acetonitrile, pyridine, and cyclopentanone – significant portions of the spectra were in the region that is smaller in wavenumber than the detection limit of the instrumentation, but could be extrapolated based on the spectrum in benzene. An example is given in Figure 9. The extrapolation was helpful for more accurate determination of quantum yield. Spectra that were even more red-shifted than those ones were not extrapolated, as their shapes and peak positions were unreliable. The impact on those quantum yields should be small because the quantum yields themselves were rather low.

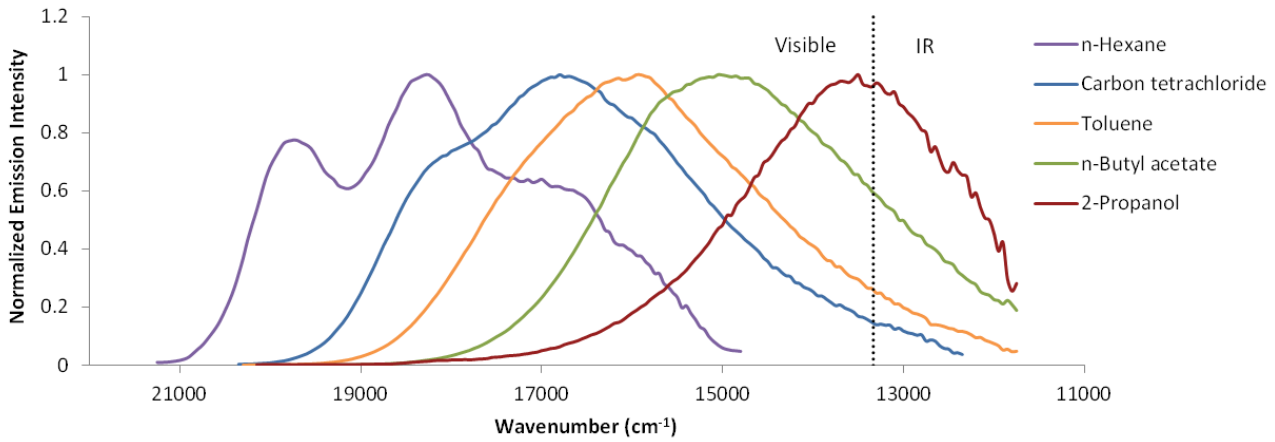

Figure 8. Corrected emission spectra of compound **1** in various solvents. The x-axis shows wavenumber going from large to small from left to right.

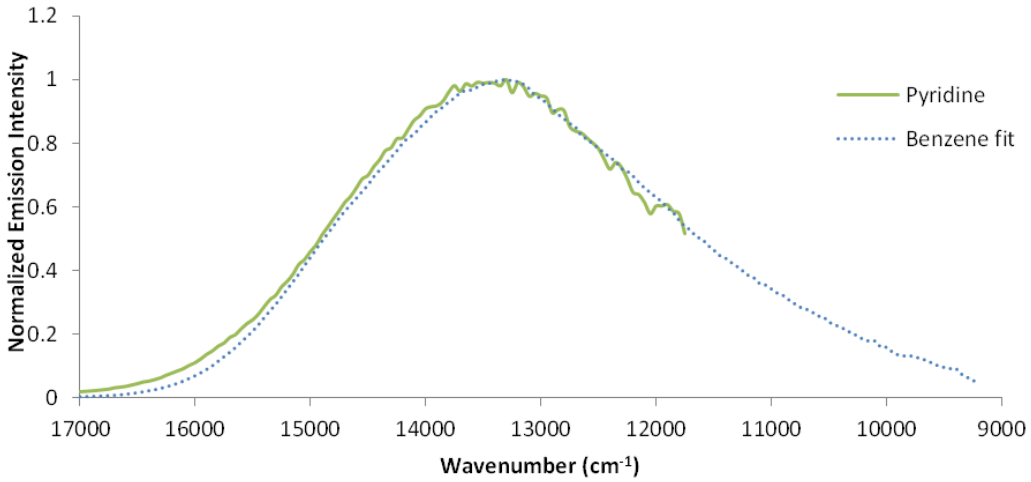

Figure 9. (Green) Corrected emission spectra of compound **1** in pyridine. (Blue, dotted) The spectrum of **1** in benzene was re-normalized and shifted to fit the peak of the pyridine curve. The overall fit was of acceptable quality.

In Figure 10, the wavenumber of maximum emission is plotted against the polarity scale $E_T(30)$ of the various solvents (also listed in Table 1; not including *n*-hexane). The alcohols conspicuously do not belong in the trend observed in the other solvents, indicating the presence of specific solvent effect that probably involves hydrogen bonding.

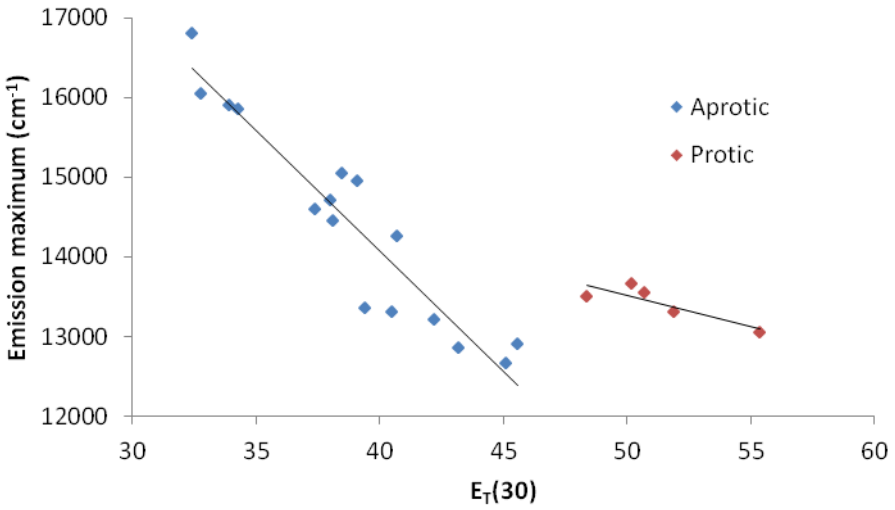

Figure 10. Emission maxima of compound **1** in various solvents against solvent polarity on the $E_T(30)$ scale. The alcohols (protic solvents) conspicuously do not belong in the trend observed in the other solvents.

The difference in wavenumbers between the absorption maximum and its corresponding emission maximum is called the Stokes shift. The general solvent effect on Stokes shift, whose mechanism was briefly outlined in the introduction, can be quantitatively described by the Lippert-Mataga equation:

$$\tilde{\nu}_{abs} - \tilde{\nu}_f = \frac{2\Delta\mu^2}{hca^3}\Delta f + C$$

where $\tilde{\nu}_{abs}$ and $\tilde{\nu}_f$ are the maxima in wavenumbers (cm^{-1}) of the absorption and emission, respectively, h is Planck's constant, c is the speed of light, a is the Onsager cavity radius, $\Delta\mu$ is the difference between the excited-state and ground-state dipole moments, C is a constant that accounts for the Stokes shift in nonpolar solvents, which is mostly due to vibrational relaxation, and Δf is the orientation polarization function of a solvent defined by

$$\Delta f = \frac{\varepsilon - 1}{2\varepsilon + 1} - \frac{n^2 - 1}{2n^2 + 1}$$

where ε and n are the dielectric constant and refractive index of the solvent, respectively. Conceptually, Δf can be thought of as a solvent polarity scale of greater theoretical interest.[1]

One may fit measured Stokes shifts (listed in Table 1) into the Lippert-Mataga equation and obtain the difference between the dipole moment of the excited state and that of the ground state, $\Delta\mu$. The plot of Stokes shift against Δf is given in Figure 11. The trend line, excluding the points representing the protic solvents, has a slope of 11266 cm^{-1}. The difference $\Delta\mu$ is thus calculated to be 15 D. Given that the ground state dipole moment is 12.5 D, the excitation more than doubles the dipole moment of the molecule. The ICT character of the transition is further confirmed.

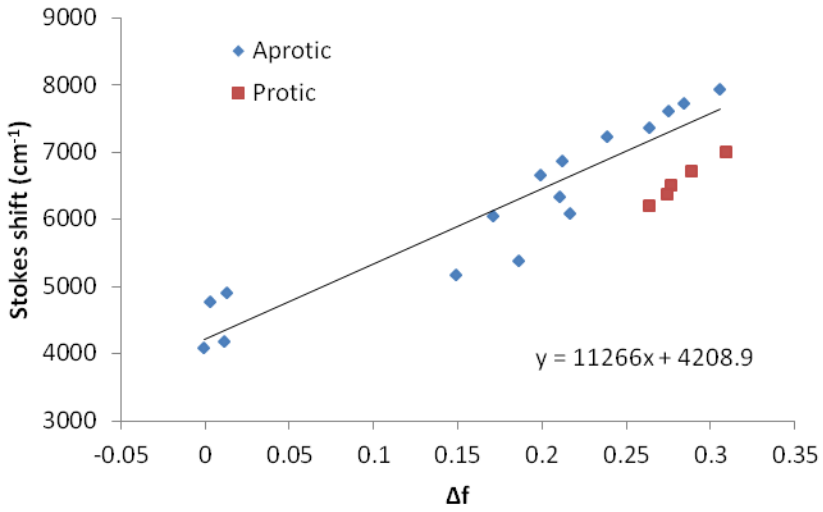

Figure 11. Lippert-Mataga plot of compound **1** in various solvents. Stokes shift is plotted against the orientation polarization function. The trend line corresponds to the aprotic solvents (blue diamonds) only.

Photophysical properties

The photophysical properties of compound **1** in different solvents are listed in Table 2. Unfortunately, the protic solvents could not be included into most of the discussion below because the lifetimes of compound **1** in them are close to the detection limit of the instrumentation, 0.1 ns.

Table 2. Photophysical properties of compound **1** in various solvents.

Solvent	Φ_f	τ (ns)	k_f (10^8 s^{-1})	k_{nr} (10^8 s^{-1})
Carbon tetrachloride	0.12	0.7	1.8	13.0
Carbon disulfide	0.32	1.4	2.3	4.9
Toluene	0.25	1.7	1.5	4.4
Benzene	0.29	1.7	1.7	4.2
Tetrahydrofuran	0.22	1.1	2.0	7.3
o-Dichlorobenzene	0.40	1.9	2.1	3.1
Ethyl acetate	0.15	0.8	1.9	10.6
n-Butyl acetate	0.27	1.5	1.8	4.9
Chloroform	0.43	1.9	2.2	3.0
Cyclopentanone	0.07	-[a]	-	-
Pyridine	0.12	0.6	1.9	14.7
Dichloromethane	0.28	1.2	2.4	6.1
Acetone	0.05	0.2	2.1	45.5
Dimethylformamide	0.01	0.2	0.9	61.6
Dimethyl sulfoxide	0.01	-[b]	-	-
Acetonitrile	0.04	0.2	1.8	48.2
Isopropanol	0.04	-[b]	-	-
n-Butanol	0.04	-[b]	-	-
n-Propanol	0.03	-[b]	-	-
Ethanol	0.02	-[b]	-	-
Methanol	0.01	-[b]	-	-

[a] Not reported because of large inaccuracy.

[b] Under the detection limit of instrumentation.

Both experimentally measured properties – quantum yield Φ_f and lifetime τ – display differences across an order of magnitude. When the two properties are plotted against the fluorescence emission maxima in different solvents (Figure 12), very similar trends can be observed: each quantity reaches a peak at the middle of the emission maxima scale ($\Phi_{f,\max}$ = 0.43 and $\tau_{\max}$ = 1.93 ns, both in chloroform at roughly 15000 cm^{-1}), and decreases toward both ends of the scale.

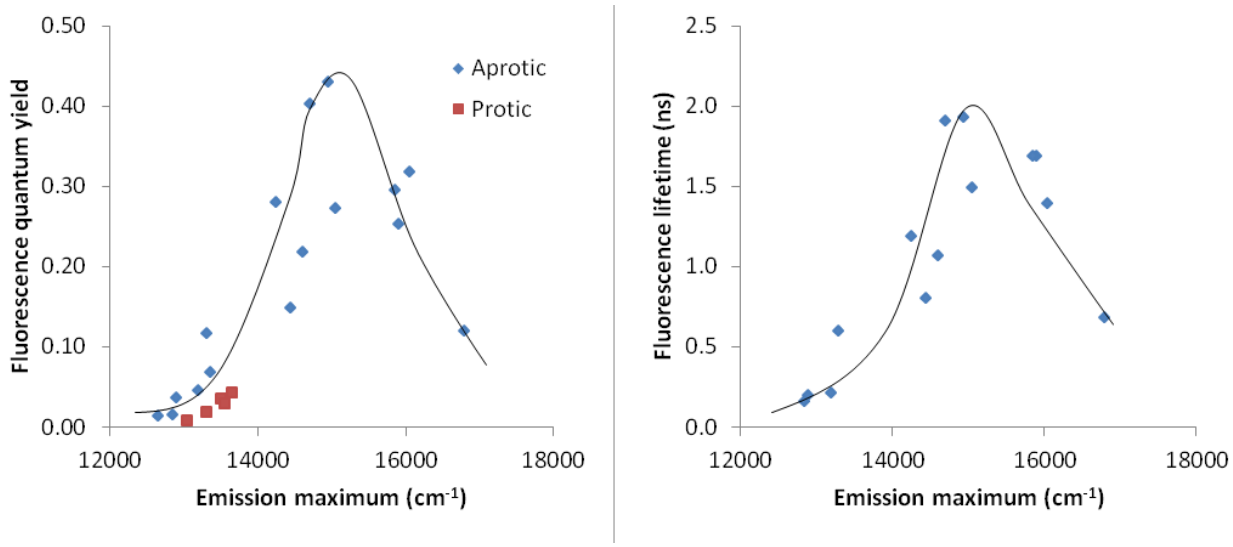

Figure 12. Fluorescence quantum yield (left) and lifetime (right) plotted against emission maximum of compound **1** in various solvents. Both plots contains an increase until about 15000 cm^{-1}, followed by a decrease.

This interesting behavior merits further investigation into the mechanism. The decay constants of both fluorescence (k_f) and non-radiative processes (k_{nr}) were calculated and plotted against the emission maxima (Figure 13).

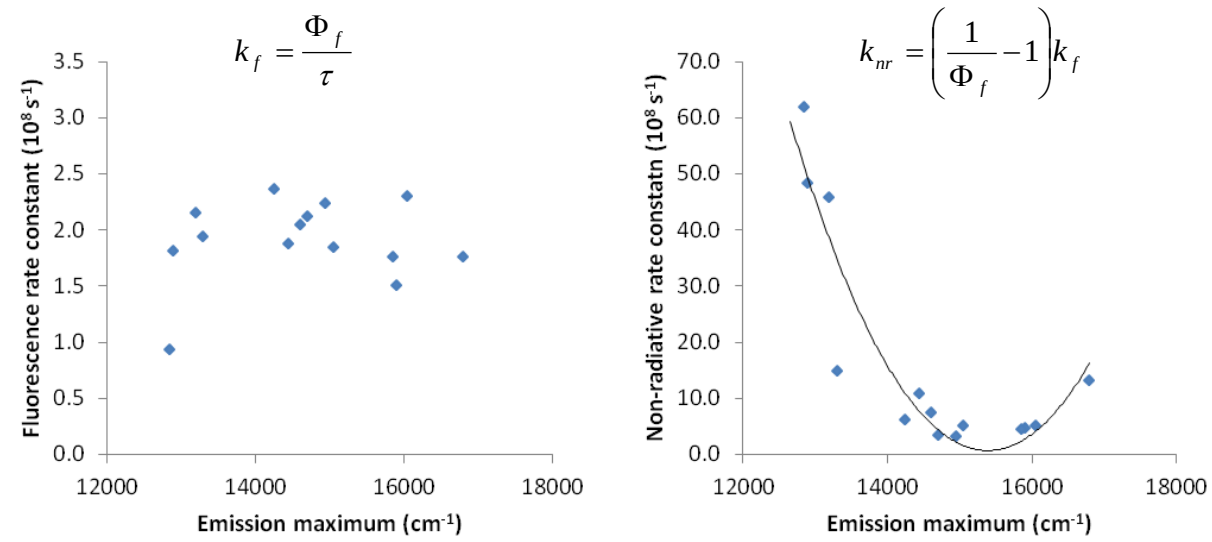

Figure 13. Decay constants of fluorescence (k_f, left) and non-radiative processes (k_{nr}, right) plotted against emission maximum of compound **1** in various solvents. Hardly any trend can be detected in the k_f plot, but the k_{nr} plot has a clear trend of a decrease until about 15000 cm^{-1}, followed by an increase.

It appears that k_f is nearly constant in all solvents, but the k_{nr} plot has a clear trend, with a minimum at the same position as the maxima in Figure 12. It is also k_{nr} that displayed an order-of-magnitude variation among the solvents. Therefore, the trend observed in quantum yield and lifetime in different solvents is mostly due to the varying rates of non-radiative processes, which compete with fluorescence at different efficiencies.

Further inquiry builds upon the knowledge that k_{nr} is the collective rate constant of two distinct non-radiative processes – internal conversion and intersystem crossing:

$$k_{nr} = k_{ic} + k_{isc}.$$

The non-monotonous overall trend of k_{nr} thus reflects the contrary behaviors of the two processes in response to changes in solvent polarity. Internal conversion is governed by the energy gap law:[11]

$$k_{ic} = C\exp(-\alpha\Delta E)$$

where ΔE is the energy gap between the two energy states in question. In our case, the states are S_1 and S_0, so ΔE is directly proportional to the emission maximum. This exponential decay fits the trend of k_{nr} in the region to the left of 15000 cm^{-1}, and thus should be the predominant factor in this region.

The region to the right of 15000 cm^{-1}, on the other hand, is dominated by the behavior of k_{isc}, which is more difficult to probe because the destination of intersystem crossing is a triplet state, for which no direct experimental information is easily available. Still, theory and calculations afforded important insight as to why k_{isc} decreases in increasingly polar solvents. A calculation was first carried out using chloroform to locate both singlet and triplet states of **1**. The energies and configurations of the states are shown in Figure 14.

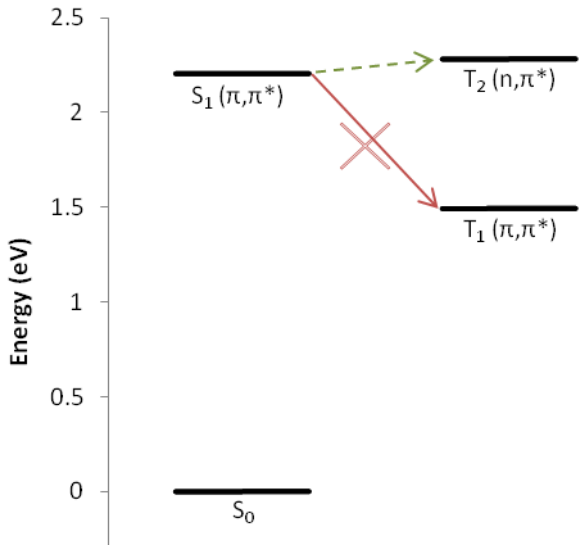

Figure 14. Energy states of compound **1** calculated in chloroform using TD-DFT. The green transition S_1 -> T_2 is allowed but requires thermal activation. The red transition S_1 -> T_1 is energetically favored but forbidden.

The rule that governs intersystem crossing is the El-Sayed's rule, which states that intersystem crossing is relatively fast between states of different orbital configuration. In other words, a π,π* singlet state readily goes through intersystem crossing to an n,π* triplet state, but not to a π,π* triplet state. As shown in Figure 14, the energetically favored S_1 -> T_1 transition of compound **1** is forbidden according to this rule. The rule may be relaxed by vibronic spin-orbit coupling, in which the S_1 and T_1 states are partially mixed through the mediation of another state (Figure 15). Nonetheless, this transition cannot proceed at high rates. The allowed transition S_1 -> T_2, on the other hand, entails an elevation in energy, and thus requires thermal activation, which is a very restrictive condition. Neither pathway is favorable, resulting in the low k_{isc} of compound **1** in chloroform.

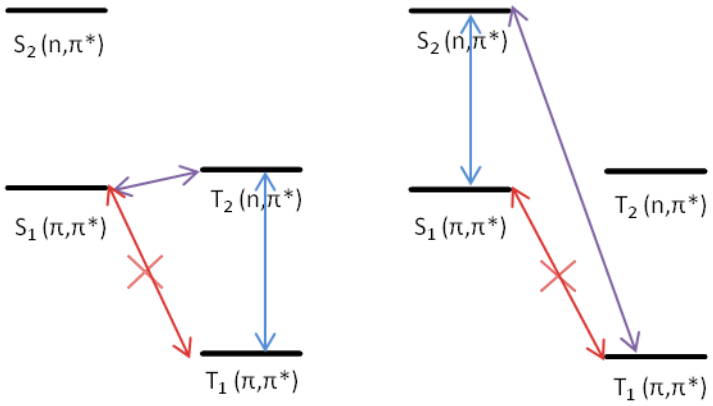

Figure 15. Coupling between S_1 and T_1 states of compound **1**. Direct spin-orbit coupling (red) is very weak, but vibronic spin-orbit coupling mediated by another state may have considerable magnitude for the compound. Two pathways are shown, with blue arrows denoting vibronic coupling and purple arrows denoting spin-orbit coupling.

A further calculation in carbon tetrachloride, along with established theory[12],suggests that under increased solvent polarity, the energy of a π,π* state decreases, but the energy of an n,π* state increases (Table 3). For compound **1**, this means that the T_2 - S_1, S_2 - S_1, and T_2 - T_1 energy gaps are all larger in more polar solvents. The enlargement of the T_2 - S_1 energy gap diminishes the possibility of thermal activation, while the enlargement of the S_2 - S_1 and T_2 - T_1 energy gaps reduces the strength of vibronic coupling. In other words, the two possible mechanisms of intersystem crossing for compound **1** both become less favorable in polar solvents. This offers a reasonable explanation for the trend of k_{isc} in different solvents.

Table 3. Energy states of compound **1** calculated in carbon tetrachloride and chloroform using TD-DFT.

Solvent	Energy above S_0 (eV)			
	T_1 (π,π*)	S_1 (π,π*)	T_2 (n,π*)	S_2 (n,π*)
Carbon tetrachloride	1.52	2.25	2.28	2.91
Chloroform	↓ 1.49	↓ 2.20	2.28	↑ 2.97

Two-Photon Absorption

The two-photon absorption of compound **1** in gas phase was studied computationally. The two-photon cross-section in gas phase was calculated to be 815 GM and 1398 GM for S_0 -> S_1 and S_0 -> S_3, respectively.[iv] Though not as impressive as the cross-sections of specially designed two-photon dyes (> 10000 GM), the values are significantly larger than those usually observed in traditional organic dyes (< 50 GM)[13], suggesting the molecule's potential use as a two-photon dye.

[iv] 1 GM = 10^{-50} cm^4 s $photon^{-1}$. The unit was named after Maria Goeppert-Mayer, the physicist who first proposed the existence of two-photon absorption.

Conclusion

Properties of a “push-pull” dye **1** were measured and calculated. The fluorescence emission maximum and Stokes shift of the dye were very sensitive to solvent polarity. Fluorescence quantum yield and lifetime showed interesting non-monotonous trends and impressively large values in chloroform. The compound has potential applications as a polarity probe, ion sensor, or two-photon dye.

References

(1) Lakowicz, J. R. *Principles of Fluorescence Spectroscopy*; 3rd ed.; Springer: New York, 2006.

(2) Connors, R. E.; Ucak-Astarlioglu, M. G. *Journal of Physical Chemistry A* **2003**, *107*, 7684.

(3) Zoto, C. A.; Connors, R. E. *Journal of Molecular Structure* **2010**, *982*, 121.

(4) Frediani, L.; Rinkevicius, Z.; Agren, H. *The Journal of Chemical Physics* **2005**, *122*, 244104.

(5) Terenziani, F.; Katan, C.; Badaeva, E.; Tretiak, S.; Blanchard-Desce, M. *Advanced Materials* **2008**, *20*, 4641.

(6) Gaussian 09, Revision A.02, M. J. Frisch, G. W. Trucks, H. B. Schlegel, G. E. Scuseria, M. A. Robb, J. R. Cheeseman, G. Scalmani, V. Barone, B. Mennucci, G. A. Petersson, H. Nakatsuji, M. Caricato, X. Li, H. P. Hratchian, A. F. Izmaylov, J. Bloino, G. Zheng, J. L. Sonnenberg, M. Hada, M. Ehara, K. Toyota, R. Fukuda, J. Hasegawa, M. Ishida, T. Nakajima, Y. Honda, O. Kitao, H. Nakai, T. Vreven, J. A. Montgomery, Jr., J. E. Peralta, F. Ogliaro, M. Bearpark, J. J. Heyd, E. Brothers, K. N. Kudin, V. N. Staroverov, R. Kobayashi, J. Normand, K. Raghavachari, A. Rendell, J. C. Burant, S. S. Iyengar, J. Tomasi, M. Cossi, N. Rega, J. M. Millam, M. Klene, J. E. Knox, J. B. Cross, V. Bakken, C. Adamo, J. Jaramillo, R. Gomperts, R. E. Stratmann, O. Yazyev, A. J. Austin, R. Cammi, C. Pomelli, J. W. Ochterski, R. L. Martin, K. Morokuma, V. G. Zakrzewski, G. A. Voth, P. Salvador, J. J. Dannenberg, S. Dapprich, A. D. Daniels, O. Farkas, J. B. Foresman, J. V. Ortiz, J. Cioslowski, and D. J. Fox, Gaussian, Inc., Wallingford CT, 2009..

(7) Dalton, a molecular electronic structure program, Release 2.0 (2005), see http://www.kjemi.uio.no/software/dalton/dalton.html.

(8) Kreher, U. P.; Rosamilia, A. E.; Raston, C. L.; Scott, J. L.; Strauss, C. R. *Organic Letters* **2003**, *5*, 3107.

(9) Austin, M.; Egan, O. J.; Tully, R.; Pratt, A. C. *Organic & Biomolecular Chemistry* **2007**, *5*, 3778.

(10) Fery-Forgues, S.; Lavabre, D. *Journal of Chemical Education* **1999**, *76*, 1260.

(11) Turro, N. J.; Ramamurthy, V.; Scaiano, J. C. *Principles of Molecular Photochemistry: An Introduction*; University Science Books, 2009.

(12) Suppan, P.; Ghoneim, N. *Solvatochromism*; Royal Society of Chemistry, 1997.

(13) Pawlicki, M.; Collins, H. A.; Denning, R. G.; Anderson, H. L. *Angewandte Chemie-International Edition* **2009**, *48*, 3244.